Direct Experimental Observation of Harmonics of Josephson Generation in the Flux-Flow Oscillator

Nickolay V. Kinev, Kirill I. Rudakov, Lyudmila V. Filippenko, and Valery P. Koshelets

***Abstract*—We present an experimental observation and a study of harmonics of radiation from a flux-flow oscillator (FFO) based on a long Josephson junction. An integrated microcircuit consisting of the FFO, the transmitting antenna and a harmonic mixer (HM) was used to provide the phase-locked emission in the terahertz (THz) range to open space. Both the FFO and the HM were made of superconductor–insulator–superconductor (SIS) trilayers based on Nb/AlO$_x$/Nb. Two independent techniques were used for detecting of the output emission: a THz Fourier transform spectrometer with a wideband detector based on an 4.2 K silicon bolometer, and a THz spectrometer based on the heterodyne SIS receiver with a high spectral resolution. The FFO spectral composition obtained using the FTS demonstrates the main Josephson frequency and clear higher harmonics. Following that, the spectral characteristics of the 2nd harmonic at a frequency of 600–670 GHz (corresponding to the main frequency of 300–335 GHz) were carefully studied with a spectral resolution better than 0.1 MHz using the SIS receiver. To our knowledge, this is the first direct high-frequency observation of Josephson harmonics carried out at the true frequency of oscillations, which is in contrast to dc measurements.**

***Index Terms*—Fourier transform infrared spectroscopy, harmonic analysis, josephson junctions, superconducting integrated circuits, terahertz radiation, transmitting antennas.**

I. Introduction

THE ac Josephson effect was discovered in 1962 [1] and was extensively studied over the next 20 years, both experimentally and theoretically. Most of the results are presented in the books completely devoted to the Josephson junctions and the effect (see, for example, [2], [3]). At present, the ac Josephson effect itself is widely used, for example, in voltage standard systems [4], [5], in high-sensitive magnetometers based on superconducting quantum interference devices [6]–[7], in rapid single-flux quantum logic systems [8]–[10], and others [11]. However, in certain applications of Josephson junctions, such as microwave detection based on the SIS mixers, the ac Josephson effect is harmful and must be eliminated by suppressing the critical current by means of a supply of the local magnetic field [12]–[14].

The Josephson equation $\hbar \cdot \partial\varphi/\partial t = 2eV_{DC}$ defines the fundamental frequency $f_{\rm J} = (2e/h)\ V_{\rm DC}$, here h is the Planck constant, e is the electron charge, and $V_{\rm DC}$ is the dc voltage. The presence of higher harmonics $f_{\rm N} = N \cdot f_{\rm J}$ with number $N \geq 2$ is already known and measured indirectly by observation of the induced steps in the current-voltage curves (IVCs) [15], [16]. A similar effect is observed for the harmonic generation of the external microwave signal in Josephson junctions [17], which is successfully used in harmonic SIS mixers [18]–[20]. Since the power of Josephson emission is rather low (typically from a few nanowatts to fractions of 1 μW [3], [21]), and taking into account that the power of higher harmonics is much lower than that of the fundamental (first) harmonic [16], these were not studied directly at a high frequency.

Recently we elaborated and tested a terahertz Josephson oscillator radiating to an open space based on the flux-flow oscillator fabricated from Nb/AlO$_x$/Nb trilayer with SIS current density in the range of 5-10 kA/cm^2 [22]–[27]. The emission to open space is provided by the transmitting slot antenna coupled with the FFO and mounted on the back surface of the semielliptical silicon lens, forming the narrow output quasioptical beam. The slot antenna is made in the niobium base electrode with a thickness of about 200 nm. The phase locking of the FFO radiation is successfully obtained using the harmonic mixer and the phase locking loop (PLL) system. Three different integrated "FFO + antenna + HM" designs were developed [22]–[24] to cover the output range of the emission from ~200 GHz up to ~750 GHz. Both direct and heterodyne detection methods were used to study the output emission to open space. A 4.2 K high-sensitive silicon bolometer was used to study the antenna characteristics in the wide range [25], [26] with the frequency definition of the output emission calculated from dc voltage of the FFO; hence, the harmonic composition could not be resolved. The superconducting integrated receiver (SIR) operating in the range roughly 500-700 GHz [28]–[29] was used for precise measurements of the FFO spectral lines radiated to open space [22], [23], with a resolution of approximately 0.1 MHz. The SIR operating bandwidth was too narrow (~35% of the central frequency) to simultaneously cover two harmonics.

In this paper, we used the FTS with a silicon bolometer-based detector to distinguish the harmonics of the FFO emission (see Section II). Following that, we studied the spectral characteristics of the second harmonic $2 \cdot f_{\rm J}$ in the SIR operating range,

Manuscript received September 16, 2021; revised December 13, 2021; accepted January 10, 2022. Date of publication January 14, 2022; date of current version January 25, 2022. The work was supported by the Russian Science Foundation under Project 17-79-20343. The development of the technology for fabrication of tunnel junctions with sub-μm dimensions was supported by the Russian Foundation for Basic Research under Project 19-52-80023. The fabrication of experimental samples was carried out using the Unique Science Unit "Cryointegral" (USU #352529), which was supported by the Ministry of Science and Higher Education of Russia under Project 075-15-2021-667. *(Corresponding author: Nickolay V. Kinev.)*

Nickolay V. Kinev, Lyudmila V. Filippenko, and Valery P. Koshelets are with the Kotel'nikov Institute of Radio Engineering and Electronics RAS, Moscow 125009, Russia (e-mail: nickolay@hitech.cplire.ru).

Kirill I. Rudakov is with the Kotel'nikov Institute of Radio Engineering and Electronics RAS, Moscow 125009, Russia, and also with the Kapteyn Astronomical Institute, University of Groningen, 9712 CP Groningen, The Netherlands.

Color versions of one or more figures in this article are available at https://doi.org/10.1109/TASC.2022.3143483.

Digital Object Identifier 10.1109/TASC.2022.3143483

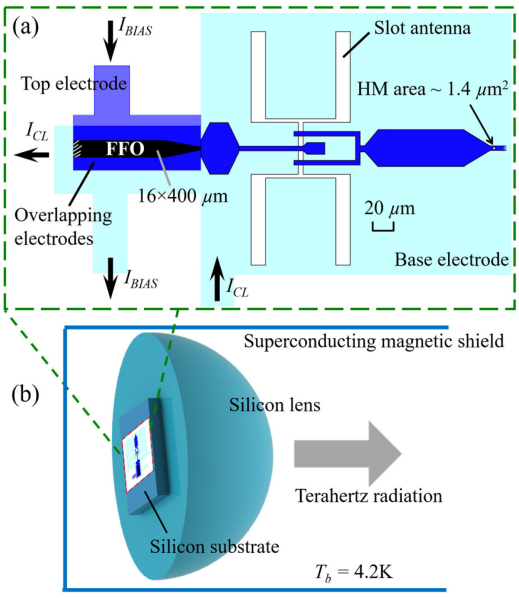

Fig. 1. (a) Layout of the oscillator integrated circuit containing the FFO, the slot antenna and the HM all interconnected by microstrip lines. (b) Sketch of lens antenna quasioptical system mounted in the 4.2 K cryostat.

while the characteristics of the main harmonic f_J out of the SIR operating range were simultaneously recorded using the feedback PLL circuit utilizing the HM (see Section III).

II. FTS Measurements

A. Design of the Oscillator

A design of the Nb/AlO$_x$/Nb-based oscillator and technology for fabrication are discussed in detail in [22], [25]. The main parts of the integrated microcircuit are presented in Fig. 1. An FFO output edge is connected to a microstrip line for feeding the transmitting lens antenna system. A small part (commonly about 5-15%) is branched to the HM to provide the feedback with the oscillator for frequency and phase locking, and also for real-time monitoring of the spectral properties of radiation. A typical output power to open space was experimentally estimated in [27] and is of the order of fractions to a few μW. The oscillator is operating in liquid helium cryostat at a bath temperature $T_b \sim$ 4.2 K, and additionally installed inside the magnetic shield due to extremely high sensitivity to external field and noise. The FFO operating point is continuously tuned in wide range by both the bias current I_{BIAS} and the control line current I_{CL} for supplying the local magnetic field.

B. Experimental Setup

In the Fourier transform spectrometer setup, we used a traditional Michelson interferometer with two flat mirrors and the beam splitter made of Mylar and oriented by 45° to the input beam (see Fig. 2). For detection, a commercially available cooled silicon bolometer by Infrared Laboratories^{TM} was used, with a noise equivalent power of 1.44·10^{-13} W/Hz$^{1/2}$ according to the specifications. The spectrometer is operating as follows: an interference pattern (mirror position, μm *vs* bolometer response, mV) as a result of the interference of beams reflected from the mirrors is recorded for the set of positions of the movable

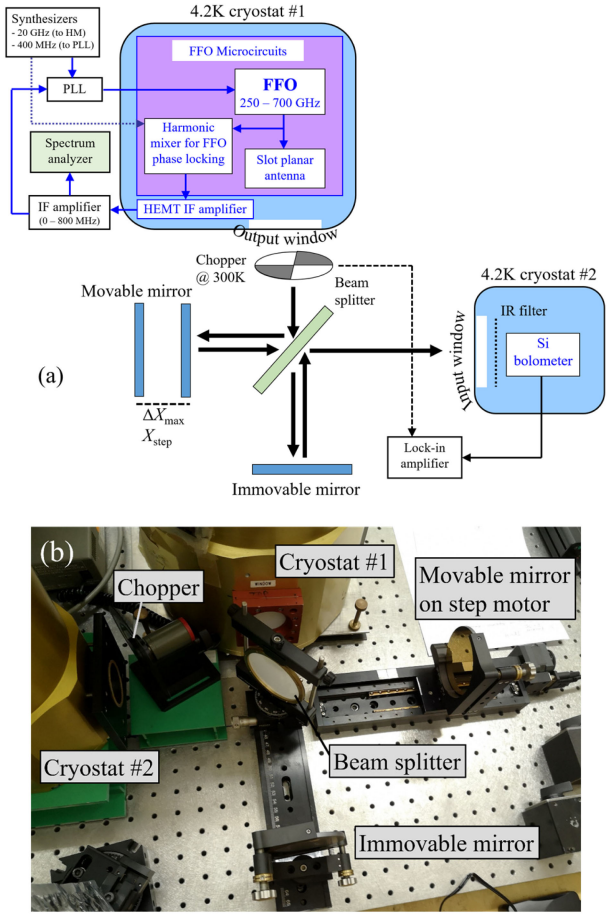

Fig. 2. (a) Block diagram of the FTS setup utilizing the Michelson interferometer layout for studying of the spectral composition of the FFO. (b) Photo of the central part of experimental setup showing the optical path of the beam, not including measuring instruments. The distance between the beam splitter and the immovable mirror ("zero-position" for the movable mirror) is 172 mm.

mirror. After that, a frequency dependence is recovered using a Fourier transform applied to the interference pattern based on the known speed of light and a step of the mirror that leads to the specific phase difference. Hence, two liquid helium cryostats were simultaneously used in the FTS setup, #1 for the emitter and #2 for the detector. A standard lock-in amplifier technique was used to read out the bolometer response, with an optical chopper at room temperature with a frequency of ~170 Hz. For dc biasing and testing of the FFO, an autonomous low-noise battery power supply (not connected to 230 V power net) was used. The equipment for the dc measurements is not shown in Fig. 2.

The maximum travel length of the movable mirror, $\Delta X_{\max}$, is 200 mm, which provides the best spectral resolution

$$\delta f \approx c \,/\, (2 \cdot \Delta X_{\max}) = 0.75\,\text{GHz},$$

where c is the speed of light. Such a resolution is redundant for the purpose of distinguishing harmonics distant by hundreds of GHz from each other. Owing to this, most measurements were carried out with a travel length of 24 mm, which leads to a spectral resolution of 6.25 GHz. The maximum frequency f_{MAX} that could be detected is defined by the minimum step of the mirror, X_{step}, which is 2.5 μm for the motor used, and

estimated as

$$f_{\max} \approx c \,/\, (4 \cdot \Delta X_{\text{step}}) = 30\,\text{THz}.$$

This expression does not take into account a factor of accuracy of restoring the spectra by Fourier transform, which is reducing f_{MAX} commonly with a coefficient 1-1.25. A frequency of 30 THz is also redundant for our study since a maximum expected frequency for detection was approximately ~1 THz due to strong losses in niobium films above 800 GHz. These losses are described by Mattis-Bardeen theory and actually set an upper frequency limit of the Josephson generation. Most measurements were carried out with a step size of 62.5 μm, which leads to the upper frequency of Fourier transform of about 1.2 THz. With the chosen parameters discussed above, the time constant of the lock-in amplifier of 300 ms and taking into account a finite motor rotation speed, the duration of one measurement at a fixed frequency was about 7 minutes. The FFO signal was phase locked during measurements providing high stability.

C. DC Results

The IVCs of the HM demonstrating the quality of the Nb/AlO$_x$/Nb trilayer are shown in Fig. 3(a). The gap voltage of the trilayer is about 2.7 mV, and the subgap resistance to the normal-state resistance ratio R_j/R_n is about 30. It is worth noting that the critical current is not suppressed for the junction presented. A set of IVCs of the FFO in wide range of magnetic fields is presented in Fig. 3(b). During the FFO dc testing, a level of the HM pumping by the FFO power was measured as follows: the HM was biased to an operating point of 2.5 mV slightly below the gap voltage, and the quasiparticle current step induced by the external emission was measured simultaneously and indicated by color at the FFO IVCs. Note that the X-axis of the FFO IVCs linearly corresponds to the frequency of the main harmonic f_J. A range of the most efficient HM pumping, which is from 350 GHz to 510 GHz for the experimental sample presented in Fig. 3, is completely defined by the design of microstrip lines and is tuned from about 200 GHz up to 750 GHz [22]–[24] with bandwidth of about 30% of central frequency.

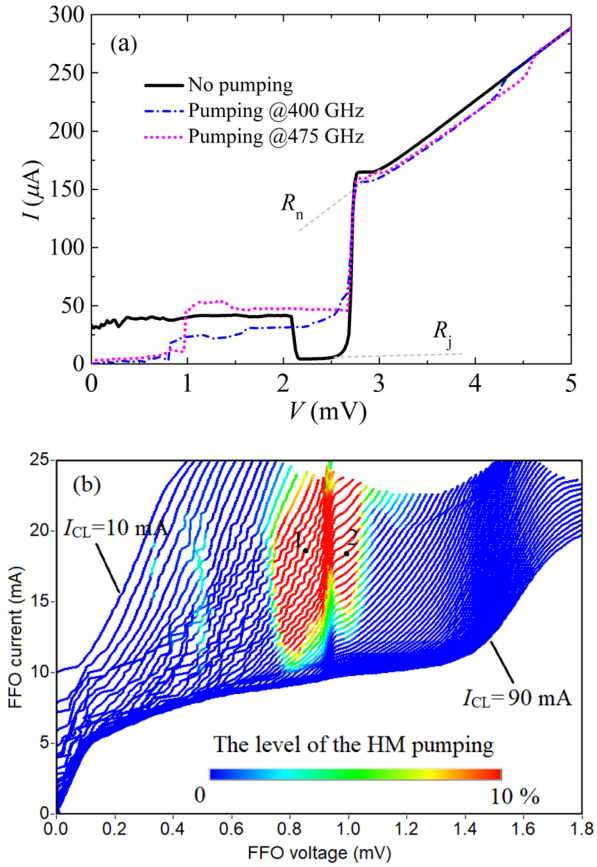

Fig. 3. (a) IVCs of Nb/AlO$_x$/Nb-based HM junction with an area of ~1.4 μm^2 on the experimental sample under study. The specific parameters are as follows: normal-state resistance $R_n = 16.2\,\Omega$, ratio R_j/R_n=32.9, gap voltage is 2.71 mV. The supplementary grey dashed curves are shown for defining the parameters. Colored dashed curves are the IVCs with pumping by the FFO emission at two different frequencies. (b) IVCs of the FFO with the dimensions 400 × 16 μm at different magnetic fields produced by the control line current from 10 mA to 90 mA. The level of the HM pumping is indicated by color as an *rf*-induced current step related to the current jump at the gap voltage; red color is pumping more than 10%. Points 1 and 2 indicate the operating points at 400 GHz and 475 GHz, correspondingly, at which the "pumped" IVCs of the HM were measured in (a).

D. High-Frequency Results

A set of wideband measurements of the FFO spectra using the FTS setup was carried out at different frequencies of the main harmonic f_J in the range from 110 GHz to 500 GHz. Furthermore, a set of measurements was carried out for certain fixed f_J. at different bias currents. A typical spectrum obtained at $f_J = 280$ GHz is presented in Fig. 4(a), with the corresponding dc operating points presented in Fig. 4(b). A clear main and the second harmonics at $f_{2ND} = 560$ GHz are demonstrated. A reasonably good signal-to-noise ratio of restoring the spectra can be noted at this operating frequency. The IVCs of the FFO at frequencies around 280 GHz corresponding to voltage of ~0.579 mV demonstrate clear Fiske steps caused by geometrical resonances inside the long junction [14], [30], [31]. The steps become completely indistinguishable at currents below 20 mA due to an increased slope, that is why the scatter-pointed IVCs are not shown in this region in Fig. 4(b). One can see that the higher bias currents (points 1 to 5) correspond to higher emission power (detector response) for both the main and the second harmonics, which is reasonable. Similar results were demonstrated for many frequencies $f_J =$ in the range of high efficiency of the transmitting antenna from ~250 GHz to ~450 GHz.

It is known that the interferometer setup can lead to artificial harmonics due to a finite travel length, phase errors and other effects. To prove that the harmonics observed by FTS are true harmonics of Josephson generation but not the artifacts of optical system, two additional techniques were used during the experiments. First, we set the FFO to the operating point at which the frequency f_J is lower than the operating range of output integrated circuit, so the signal of the main harmonic could not come out of the junction reflecting from its edge. At the same time, the higher harmonics $f_{2ND} = 2f_J$, and, in some cases, $f_{3RD} = 3f_J$ were permitted by the output microstrip lines and the transmitting antenna, and hence were detected by the FTS. The results for certain frequencies are presented in Fig. 5, where higher harmonics are clearly demonstrated *with the absence of the main harmonic*. One should note that there is a much worse signal-to-noise ratio compared to results in Fig. 4(a), as the power of higher harmonics is approximately one-two orders of magnitude lower than that of the main harmonic. Another point

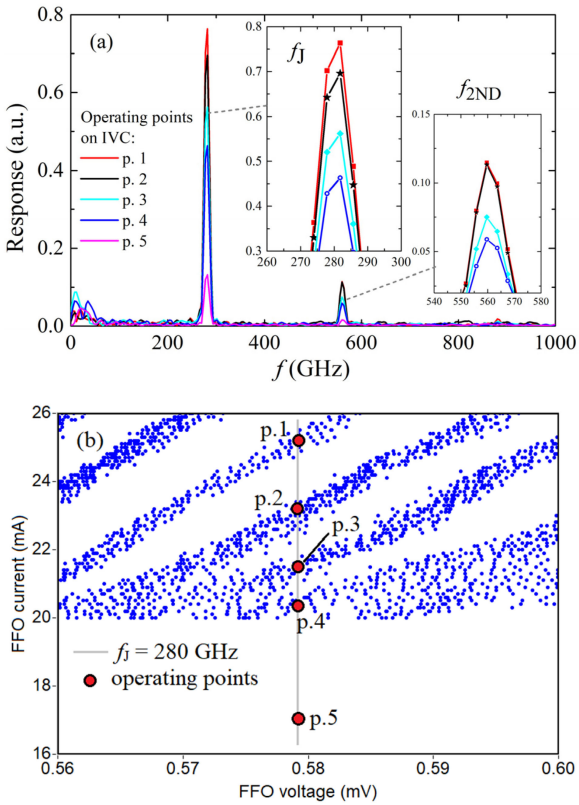

Fig. 4. (a) Spectra of the FFO output emission at $f_J = 280$ GHz obtained by the FTS, at different operating points 1-5 specified in (b). The insets are shown in larger scale for clarity, to distinguish curves close to each other. (b) IVCs of the FFO presented by scatter points around voltage of 0.579 mV corresponding to $f_J = 280$ GHz. Operating points 1-5 are located at different Fiske steps. Region of IVCs is not shown below 20 mA.

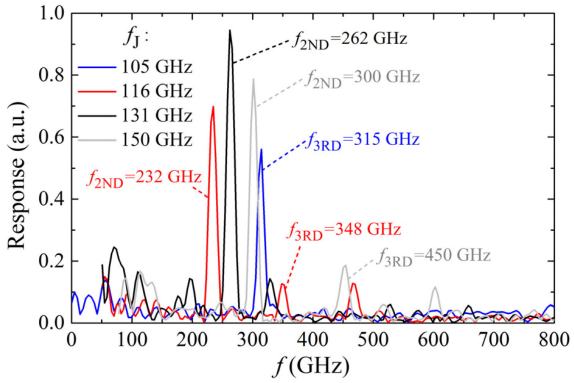

Fig. 5. Spectra of the FFO output emission at a set of f_J out of the operating range of the chip design, obtained by the FTS. Only higher harmonics are observed and marked on the graph.

to note is presence of the peaks at frequencies corresponding to 4th harmonics of f_J or, the same, 2nd harmonics of f_{2ND}: see, for example, in Fig. 5 the peak at ~460 GHz for $f_J = 116$ GHz, and the peak at 600 GHz for $f_J = 150$ GHz. The magnitude of these peaks is almost the same as that of 3rd harmonics. We suppose that these peaks in particular are the artifacts of the optical system related to additional modes in the interferometer and not related to Josephson generation.

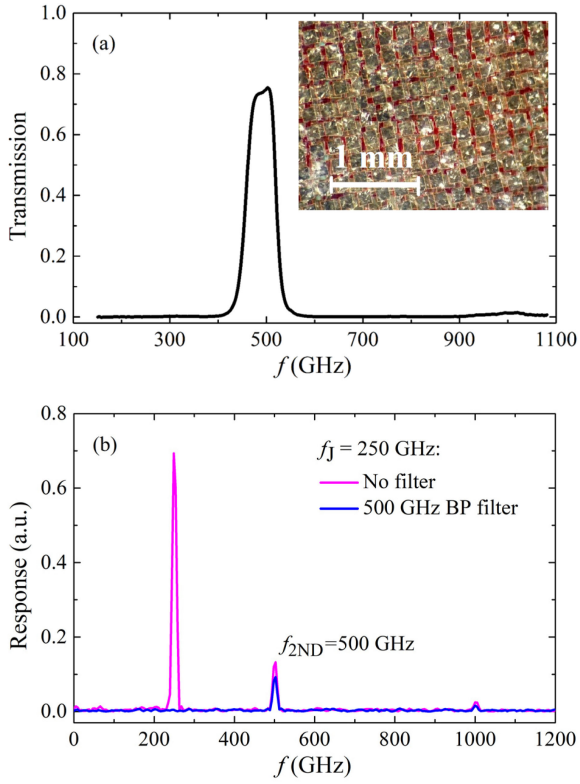

Fig. 6. (a) Specification of 500 GHz BP filter given by the manufacturer, with a micrograph shown in the inset. (b) Spectra of the FFO output emission at $f_J = 250$ GHz obtained by the FTS, using the original technique (red curve) and with the additional BP filter (blue curve).

Another technique is using a bandpass (BP) filter for one of the harmonics. A commercially available 500 GHz narrowband multi-layered mesh filter produced by QMC Instruments^{TM} was used, having a frequency specification presented in Fig. 6(a). We set the FFO to operating point of $f_J = 250$ GHz and observed a 2nd harmonic at $f_{2ND} = 500$ GHz as discussed above (red curve in Fig. 6(b)). Following that, we installed the BP filter at the output window with the emitter and clearly observed only 2nd harmonics while the main one was filtered (blue curve in Fig. 6(b)). This experiment is the evidence of true Josephson harmonics, otherwise the 2nd harmonics would not be observed without the first one. One should note a small peak at 1000 GHz corresponding to 4th harmonics, which is observed both with and without the filter. Since the BP filter cannot allow this frequency, and taking into account that niobium films obviously cannot operate at so high frequencies due to losses (Mattis-Bardeen theory), the peak at 1000 GHz is evident artifact generated by the interferometer setup.

III. SIS Receiver Measurements

A. Experimental Setup

As we ensured the presence of true Josephson harmonics radiated to open space, we studied the spectral characteristics of the first two harmonics simultaneously with high spectral resolution utilizing the superconducting integrated receiver [14], [28], [29]. The experimental setup is shown in Fig. 7. Owing to the fact that the operating range of the SIR (roughly 500–700 GHz)

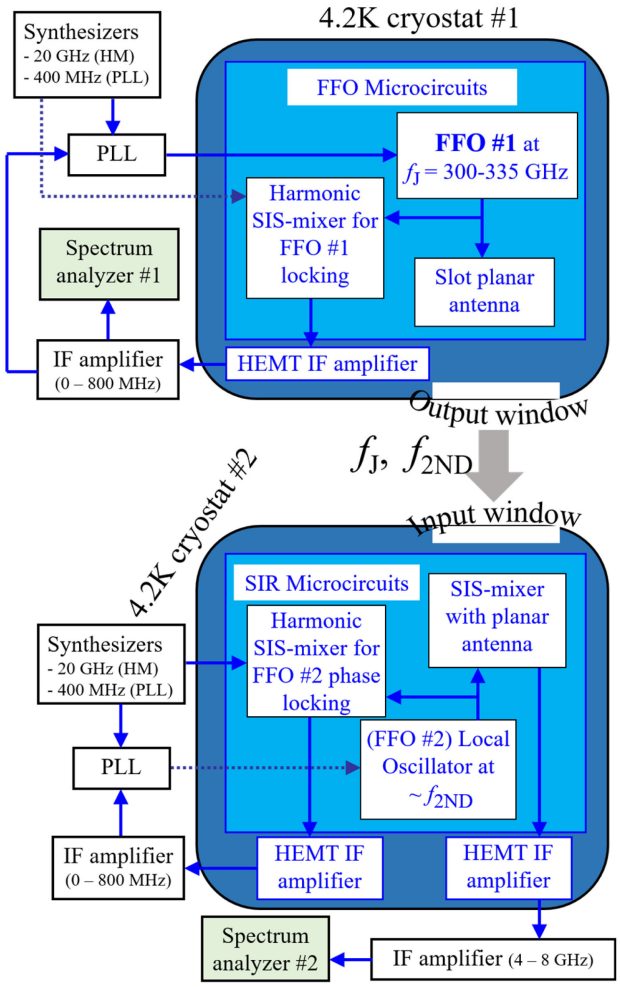

Fig. 7. Block diagram of the experimental setup for studying the emission spectral lines of both the main and second harmonics of the FFO simultaneously with resolution of 0.1 MHz.

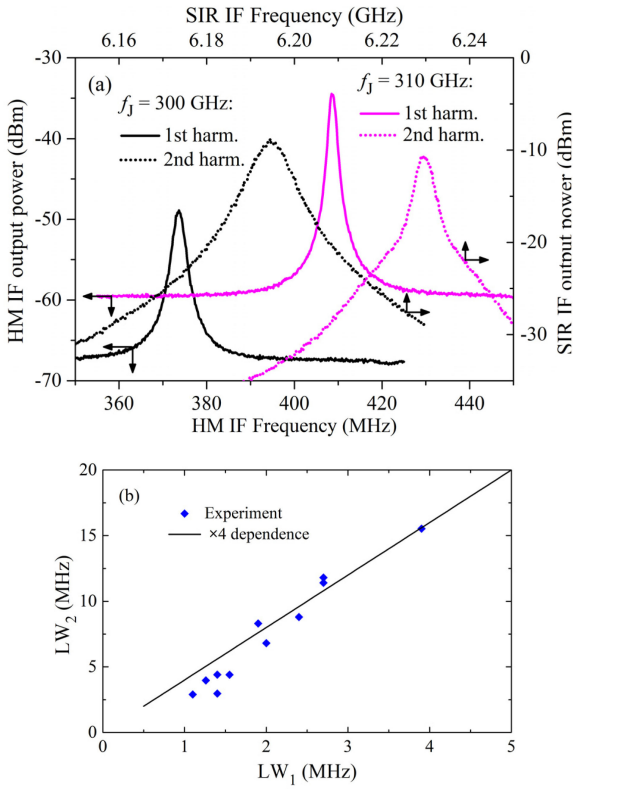

Fig. 8. (a) Power spectra of the first and second harmonics of the FFO at two frequencies f_J = 300, 310 GHz. The span for both (top and bottom) horizontal axes is the same and equals to 100 MHz. The defined linewidths are as follows: LW_1 = 2.4 MHz, LW_2 = 8.8 MHz at 300 GHz, and LW_1 = 1.55 MHz, LW_2 = 4.4 MHz at 310 GHz. (b) Linewidth of the first and second harmonics of the FFO obtained at f_J in the range from 300 GHz to 335 GHz. A theoretical straight line LW_2=4·LW_1 is drawn for assistance.

is much narrower than that of the bolometer-based detector in the FTS, only one harmonic, f_{2ND}, can be detected by the SIR simultaneously, while the main harmonic at f_J is studied in parallel using the HM in the PLL circuit. Hence, two spectrum analyzers (SA) are used in such a complex setup (see Fig. 7): SA #1 for recording the spectra of the main harmonic in the HM intermediate frequency (IF) range of 0-800 MHz, and SA #2 for recording the spectra of the second harmonic in the SIS-mixer IF range of 4-8 GHz. IF amplifiers are based on high electron mobility transistors (HEMT) at a temperature of 4.2 K.

B. Results

The second harmonic was successfully detected and recorded by the SA #2, for the set of main frequencies in the range from 300 GHz to 335 GHz, corresponding to f_{2ND} in the range of 600–670 GHz. The typical spectra of both the first and second harmonics are presented in Fig. 8(a) for the main frequency of 300 GHz and 310 GHz. One should note that the signal of the second harmonic detected using this technique is the convolution of true spectra and the spectra of the SIR local oscillator (LO), which is also based on the FFO (#2 in Fig. 7). Theoretically, the linewidth of the N-th harmonic (LW_N) defined at a half power of the peak is N^2 times larger than that of the first one (LW_1) for the case of wideband fluctuations (spectral density of voltage noise $S(\omega)$ is nearly constant in the range $0 < \omega < LW_1$), which means that $LW_2 = 4 \cdot LW_1$ (see chapter 4 in the book [3]). The coefficient LW_2/LW_1 obtained experimentally for most operating points is close to 4; a certain deviation can be still noted for $LW_1 < 2$ MHz. An accurate calculation of the signal convolutions of the harmonics and LO is a different task for a separate paper. In Fig. 8(b), a summary of LW's for all studied spectra (diamonds) and the theoretical value $LW_2/LW_1 = 4$ (solid line) are presented.

IV. Conclusion

A direct observation of the Josephson harmonics at terahertz frequencies is demonstrated for the first time, by different techniques: using the wideband FTS and the heterodyne receiver. Clear harmonics up to $N = 3$ are detected by the FTS, and the spectral characteristics (shape and linewidth) of the 2nd harmonic are measured by the receiver. A ratio of linewidth of the second-to-first harmonics of appriximately 4 is obtained, which corresponds well to theoretical value of N^2 taking into account a deviation of the LO spectra from δ-function.

REFERENCES

[1] B. D. Josephson, "Possible new effects in superconductive tunnelling," *Phys. Lett.*, vol. 1, no. 7, pp. 251–253, Jul. 1962, doi: 10.1016/0031-9163(62)91369-0.

[2] A. Barone and G. Paterno, *Physics and Applications of the Josephson Effect*. Hoboken, NJ, USA: Wiley, 1982, doi: 10.1002/352760278X.

[3] K. K. Likharev, *Dynamics of Josephson Junctions and Circuits*, 3rd ed. New York, NY, USA: Gordon & Breach Science, 1996.

[4] C. A. Hamilton, C. J. Burroughs, and S. P. Benz, "Josephson voltage standard-a review," *IEEE Trans. Appl. Supercond.*, vol. 7, no. 2, pp. 3756–3761, Jun. 1997, doi: 10.1109/77.622234.

[5] C. J. Burroughs *et al.*, "NIST 10 v programmable Josephson voltage standard system," *IEEE Trans. Instrum. Meas.*, vol. 60, no. 7, pp. 2482–2488, Jul. 2011, doi: 10.1109/TIM.2010.2101191.

[6] A. Barone, *Principles and Applications of Superconducting Quantum Interference Devices*. Singapore: World Scientific Co. Pte Ltd., 1992, doi: 10.1142/1607.

[7] J. Clarke and A. I. Braginski, *The SQUID Handbook: Fundamentals and Technology of SQUIDs and SQUID Systems*, vol. 1. Weinheim, Germany: Wiley VCH, 2004.

[8] S. V. Polonsky *et al.*, "New RSFQ circuits (Josephson junction digital devices)," *IEEE Trans. Appl. Supercond.*, vol. 3, no. 1, pp. 2566–2577, Mar. 1993, doi: 10.1109/77.233530.

[9] O. A. Mukhanov, S. V. Rylov, D. V. Gaidarenko, N. B. Dubash, and V. V. Borzenets, "Josephson output interfaces for RSFQ circuits," *IEEE Trans. Appl. Supercond.*, vol. 7, no. 2, pp. 2826–2831, Jun. 1997, doi: 10.1109/77.621825.

[10] A. V. Ustinov and V. K. Kaplunenko, "Rapid single-flux quantum logic using π-shifters," *J. Appl. Phys.*, vol. 94, no. 8, pp. 5405–5407, Sep. 2003, doi: 10.1063/1.1604964.

[11] A. I. Braginski, "Superconductor electronics: Status and Outlook," *J. Supercond. Novel Magnetism*, vol. 32, pp. 23–44, Nov. 2018, doi: 10.1007/s10948-018-4884-4.

[12] S. Haas, C. E. Honingh, D. Hottgenroth, K. Jacobs, and J. Stutzki, "Low noise broadband tunerless waveguide sis receivers for 440–500 GHz and 630–690 GHz," *J. Infrared, Millimeter, Terahertz Waves*, vol. 17, no. 3, pp. 493–506, Mar. 1996, doi: 10.1007/BF02088024.

[13] J. W. Kooi, G. Chattopadhyay, M. Thielman, T. G. Phillips, and R. Schieder, "Noise stability of SIS receivers," *J. Infrared, Millimeter, Terahertz Waves*, vol. 21, no. 5, pp. 689–716, May 2000, doi: 10.1023/A:1026452324545.

[14] V. P. Koshelets and S. V. Shitov, "Integrated superconducting receivers," *Supercond. Sci. Technol.*, vol. 13, no. 5, pp. R53–R69, 2000, doi: 10.1088/0953-2048/13/5/201.

[15] D. B. Sullivan, R. L. Peterson, V. E. Kose, and J. E. Zimmerman, "Generation of harmonics and subharmonics of the Josephson oscillation," *J. Appl. Phys.*, vol. 41, no. 12, pp. 4865–4873, Apr. 1970, doi: 10.1063/1.1658554.

[16] R. S. Likes and C. M. Falco, "Power spectrum of radiation from a Josephson junction," *J. Appl. Phys.*, vol. 48, no. 12, pp. 5370–5371, 1977, doi: 10.1063/1.323541.

[17] D. G. McDonald, V. E. Kose, K. M. Evenson, J. S. Wells, and J. D. Cupp, "Harmonic generation and submillimeter wave mixing with the Josephson effect," *Appl. Phys. Lett.*, vol. 15, no. 4, pp. 121–122, Aug. 1969, doi: 10.1063/1.1652930.

[18] P. Kittara, S. Withington, and G. Yassin, "Theoretical and numerical analysis of very high harmonic superconducting tunnel junction mixers," *J. Appl. Phys.*, vol. 101, no. 2, pp. 024508–1–024508–7, Jan. 2007, doi: 10.1063/1.2424407.

[19] K. V. Kalashnikov, A. V. Khudchenko, A. B. Baryshev, and V. P. Koshelets, "Harmonic mixer based on superconductor-insulator-superconductor tunnel junction," *J. Commun. Technol. Electron.*, vol. 56, no. 6, pp. 699–707, doi: 10.1134/S106422691106009X.

[20] K. V. Kalashnikov, A. A. Artanov, G. de Lange, and V. P. Koshelets, "Investigation of the harmonic mixer and low-frequency converter regimes in a superconducting tunnel junction," *IEEE Trans. Appl. Supercond.*, vol. 28, no. 4, Feb. 2018, Art. no. 2400105, doi: 10.1109/TASC.2018.2803043.

[21] H. Fack and V. Kose, "Maximal output power of point-contact Josephson junctions," *J. Appl. Phys.*, vol. 42, no. 1, pp. 322–323, 1971, doi: 10.1063/1.1659594.

[22] N. V. Kinev, K. I. Rudakov, L. V. Filippenko, A. M. Baryshev, and V. P. Koshelets, "Flux-flow Josephson oscillator as the broadband tunable terahertz source to open space," *J. Appl. Phys.*, vol. 125, no. 15, pp. 151603–1–151603–7, Mar. 2019, doi: 10.1063/1.5070143.

[23] N. V. Kinev, K. I. Rudakov, L. V. Filippenko, A. M. Baryshev, and V. P. Koshelets, "An antenna with a feeder for a superconducting terahertz Josephson oscillator with phase locking," *J. Commun. Technol. Electron.*, vol. 64, no. 10, pp. 1081–1086, Oct. 2019, doi: 10.1134/S1064226919090122.

[24] N. V. Kinev, K. I. Rudakov, A. M. Baryshev, and V. P. Koshelets, "Slot lens antenna based on thin Nb films for the wideband Josephson terahertz oscillator," *Phys. Solid State*, vol. 60, no. 11, pp. 2173–2177, Nov. 2018, doi: 10.1134/S1063783418110112.

[25] N. V. Kinev, K. I. Rudakov, L. V. Filippenko, A. M. Baryshev, and V. P. Koshelets, "Source radiating to open space based on the superconducting flux-flow oscillator: Development and characterization," *IEEE Trans. Terahertz Sci. Technol.*, vol. 9, no. 6, pp. 557–564, Nov. 2019, doi: 10.1109/TTHZ.2019.2941401.

[26] N. V. Kinev, K. I. Rudakov, L. V. Filippenko, and V. P. Koshelets, "A terahertz source of radiation to open space based on a long Josephson junction," *Phys. Solid State*, vol. 62, no. 9, pp. 1543–1548, Sep. 2020, doi: 10.1134/S1063783420090140.

[27] N. V. Kinev, K. I. Rudakov, L. V. Filippenko, A. M. Baryshev, and V. P. Koshelets, "Terahertz spectroscopy of gas absorption using the superconducting flux-flow oscillator as an active source and the superconducting integrated receiver," *Sensors*, vol. 20, no. 24, 2020 Art. no. 7267, doi: 10.3390/s20247267.

[28] G. Lange *et al.*, "Development and characterization of the superconducting integrated receiver channel of the TELIS atmospheric sounder," *Supercond. Sci. Technol.*, vol. 23, no. 4, Mar. 2010, Art. no. 045016, doi: 10.1088/0953-2048/23/4/045016.

[29] V. P. Koshelets *et al.*, "Superconducting integrated terahertz spectrometers," *IEEE Trans. Terahertz Sci. Technol.*, vol. 5, no. 4, pp. 687–694, Jun. 2015, doi: 10.1109/TTHZ.2015.2443500.

[30] V. P. Koshelets *et al.*, "Phase locked 270–440 GHz local oscillator based on flux flow in long Josephson tunnel junctions," *Rev. Sci. Instruments*, vol. 71, no. 1, pp. 289–293, Jan. 2000, doi: 10.1063/1.1150195.

[31] V. P. Koshelets *et al.*, "Line width of Josephson flux flow oscillators," *Physica C*, vol. 372–376, no. 1, pp. 316–321, Aug. 2002, doi: 10.1016/S0921-4534(02)00659-7.